

Development Plus Kinetic and Mechanistic Studies of a Prototype Supported-Nanoparticle Heterogeneous Catalyst Formation System in Contact with Solution: Ir(1,5-COD)Cl/ γ -Al₂O₃ and Its Reduction by H₂ to Ir(0)_n/ γ -Al₂O₃

Joseph E. Mondloch,[†] Qi Wang,[‡] Anatoly I. Frenkel[‡] and Richard G. Finke^{†*}

[†]Department of Chemistry, Colorado State University, Fort Collins, CO 80523

[‡]Department of Physics, Yeshiva University, New York, NY 10016

Additional Results and Discussion

EXAFS INN Fitting for the Ir(1,5-COD)Cl/ γ -Al₂O₃ Precatalyst, [Ir(1,5-COD)Cl]₂ and [Ir(1,5-COD) μ -OCH₃]₂ Reference Compounds as Well as the Ir(0)₋₉₀₀/ γ -Al₂O₃ Catalyst

Data processing and analysis were performed using the IFEFFIT package. The EXAFS analysis was done by fitting the theoretical FEFF6 signals to the experimental data in r-space. All the fitted data was limited to the first nearest neighbor (1NN)

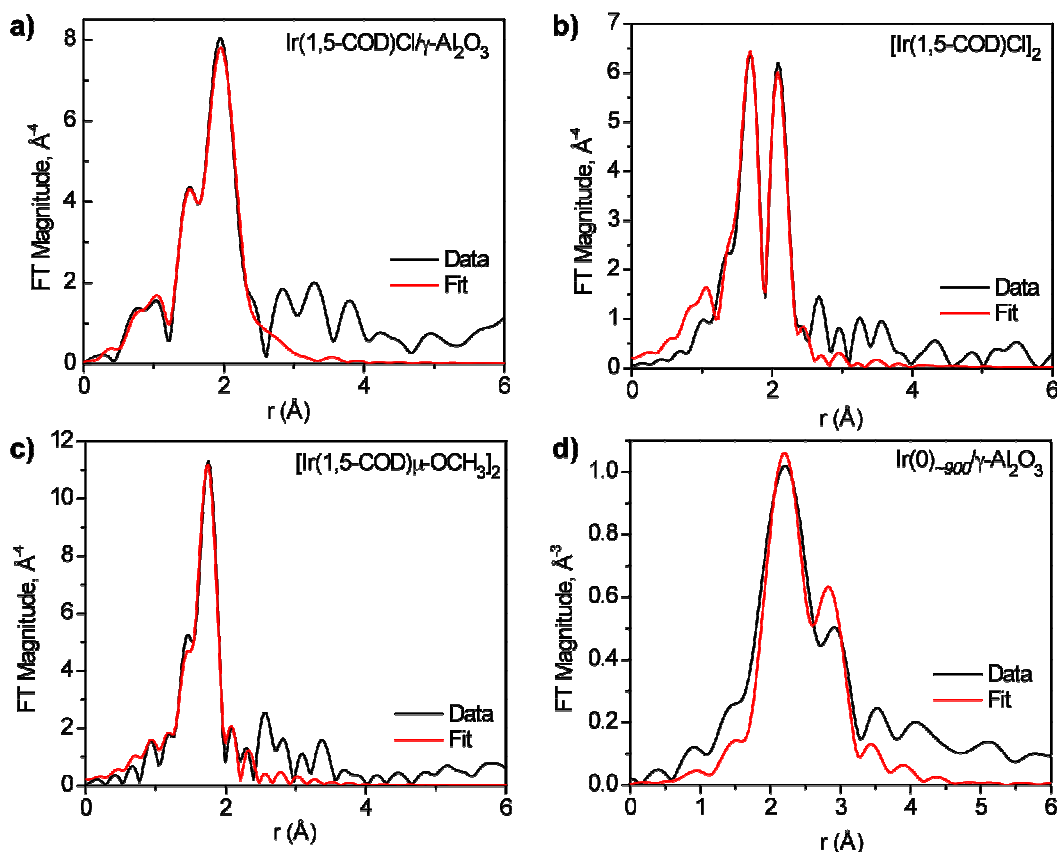


Figure S1. Fourier transform magnitudes of the Ir L₃-edge data (black) and their associated fits (red) for: (a) the Ir(1,5-COD)Cl/ γ -Al₂O₃ precatalyst (k^3 -weighting, k range from 2 to 11.5 Å⁻¹); (b) [Ir(1,5-COD)Cl]₂ (k^3 -weighting, k range from 2.5 to 14.5 Å⁻¹); (c) [Ir(1,5-COD) μ -OCH₃]₂ (k^3 -weighting, k -range from 2.5 to 16 Å⁻¹) and (d) Ir(0)₋₉₀₀/ γ -Al₂O₃ (k^2 -weighting = 2, k range from 2.5 to 9.3 Å⁻¹).

contributions. The passive electron factors, S_0^2 , were found to be 0.80 by fits to standard Iridium black, and thus fixed for further analysis of the $\text{Ir}(0)_n$ nanoparticles. The parameters describing the electronic properties (e.g., correction to the photoelectron energy origin) and local structure environment (coordination numbers N , bond lengths R and their mean squared disorder parameters σ^2) around the absorbing atoms were varied during the fitting. The molecular nature of the $\text{Ir}(1,5\text{-COD})\text{Cl}/\gamma\text{-Al}_2\text{O}_3$ precatalyst, as well as the reference compounds $[\text{Ir}(1,5\text{-COD})\text{Cl}]_2$ and $[\text{Ir}(1,5\text{-COD})\mu\text{-OCH}_3]_2$ have significant differences in electronic structure compared to $\text{Ir}(0)$ black. We obtained $S_0^2 = 1$ from the fit to the reference compound $[\text{Ir}(1,5\text{-COD})\mu\text{-OCH}_3]_2$ while constraining $N_{\text{Ir-C}}$ and $N_{\text{Ir-O}} = 2$ based on its known structure, and then fixed $S_0^2 = 1$ in the fits of the precatalyst as well as the $[\text{Ir}(1,5\text{-COD})\text{Cl}]_2$ reference compound. The photoelectron path between Ir and its carbon nearest neighbors (Ir-C) was used to simulate both the Ir-C and Ir-O contributions, as C and O are not readily distinguishable by the EXAFS analysis. Additionally, a physically reasonable constraint holding the $\text{CN}(\text{Ir-C})$ and $\text{CN}(\text{Ir-Cl})$ equal to 6 was applied in the EXAFS fits for the precatalyst as well as $[\text{Ir}(1,5\text{-COD})\text{Cl}]_2$. Furthermore, fits to the $\text{Ir}(1,5\text{-COD})\text{Cl}/\gamma\text{-Al}_2\text{O}_3$ precatalyst were based on the fixed f^2 for both Ir-C and Ir-Cl , found from fitting the $[\text{Ir}(1,5\text{-COD})\text{Cl}]_2$ structure. The data obtained from the fits is given in Table 1 of the main text.

Additional TEM Imaging and Particle Size Histograms for the $\text{Ir}(0)_{\sim 900}/\gamma\text{-Al}_2\text{O}_3$ Heterogeneous Nanoparticle Catalyst

Shown below are additional TEM images for the $\text{Ir}(0)_{\sim 900}/\gamma\text{-Al}_2\text{O}_3$ prototype catalyst and that correspond to Figure 4 of the main text. The additional images help further reveal the catalyst morphology.

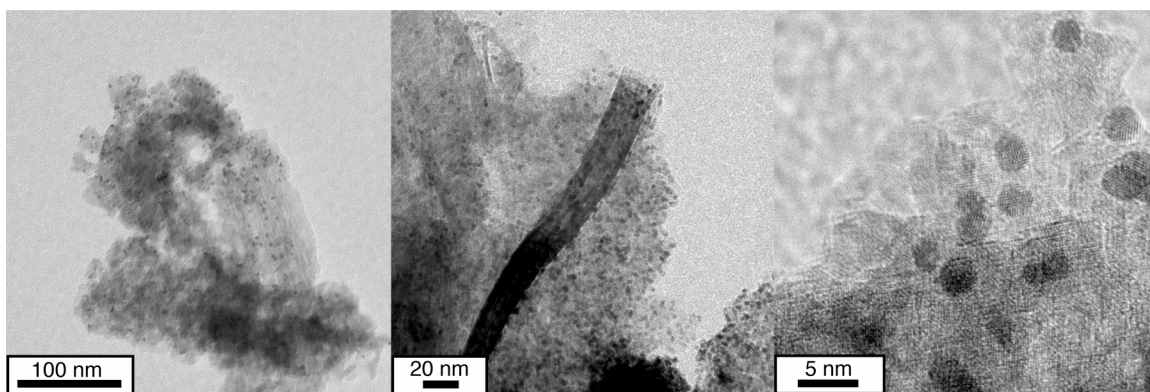


Figure S2. Additional TEM imaging for the $\text{Ir}(0)_{\sim 900}/\gamma\text{-Al}_2\text{O}_3$ heterogeneous catalyst. These images further reveal the catalyst morphology then is seen in Figure 4 of the main text.

Control Testing for H_2 Gas-to-Solution Mass Transfer Limitations (MTL)

H_2 gas-to-solution MTL have been observed to cause undesired effects such as bulk $\text{Rh}(0)_n$ in the formation of Rh polyoxoanion stabilized nanoparticles.ⁱ This is due to the competing effects between diffusive aggregation and autocatalytic surface growth.ⁱ To test whether H_2 gas-to-solution MTL is affecting the observed kinetics provided in the main text, stirring speed dependent plots were performed, a classic test for the presence

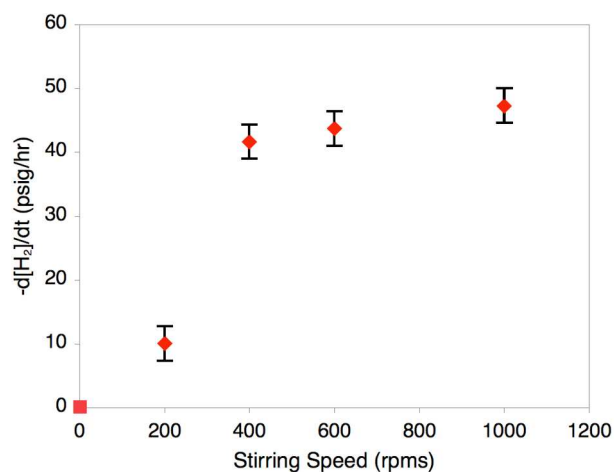


Figure S3. Stirring speed dependence for the $\text{Ir}(0)_{\sim 900}/\gamma\text{-Al}_2\text{O}_3$ heterogeneous nanoparticle formation reaction.

of MTL.ⁱ If H_2 going into solution (i.e., MTL) is part of the overall rate-determining step, then the rate will be dependent on the stirring speed of the reaction.

Each of four “standard condition” reactions was prepared as described in the experimental section of the main text with the following exception. Stirring was carried out at the appropriate speeds (200-1000 rpms). Note that the “0,0” point in Figure S4 is not an experimentally observed data point, but one that should be true physically. The data in Figure S3 show that at 600 rpms stirring speed, where our experiments were performed, the reaction rate is largely independent of the stirring rate. For example, when the stirring speed is increased from 600 to 1000 rpms, the reaction rate increases only 3.5 parts in 47 corresponding to only a 7.5% increase in the rate of the reaction. This introduces an error of $\leq 15\%$ into the resultant rate constants, an error less than that we typically see in the $\text{Ir}(0)_{\sim 900}/\gamma\text{-Al}_2\text{O}_3$ heterogeneous nanoparticle catalyst formation kinetics (Table 2) and thus negligible. In short, the stirring rate MTL controls in Figure S3 demonstrate that MTL are negligible in the present case and under our experimental conditions in our specific experimental apparatus detailed in the Experimental section of the main text.

Testing the Cyclohexene Reporter Reaction for the Desired Zero-Order [Cyclohexene] Dependence

Six “standard condition” reactions were independently prepared as described in the Experimental section of the main text. In each separate experiment the cyclohexene concentration was varied, and the acetone concentration was adjusted to compensate for the amount of cyclohexene present so that the final solution volume was always 3.0 mL. For example, if 0.2 mL of cyclohexene was used 2.8 mL of acetone would be used bringing the total volume to 3.0 mL.

The cyclohexene reporter reaction must be fast (see Scheme 2 of the main text), in comparison to the $\text{Ir}(0)_{\sim 900}/\gamma\text{-Al}_2\text{O}_3$ heterogeneous nanoparticle catalyst formation steps k_1 and k_2 , if the reporter reaction is working properly. This requirement is experimentally testable by looking at the [cyclohexene] dependence of the reaction, the results of which are shown in Figure S4. Saturation kinetics are observed by the time 1.65 M cyclohexene

is reached, the amount used in the present studies. Hence, the rate of cyclohexene hydrogenation is indeed fast relative to k_1 and k_2 , the desired nanoparticle formation steps whose kinetics are, therefore, actually being measured.

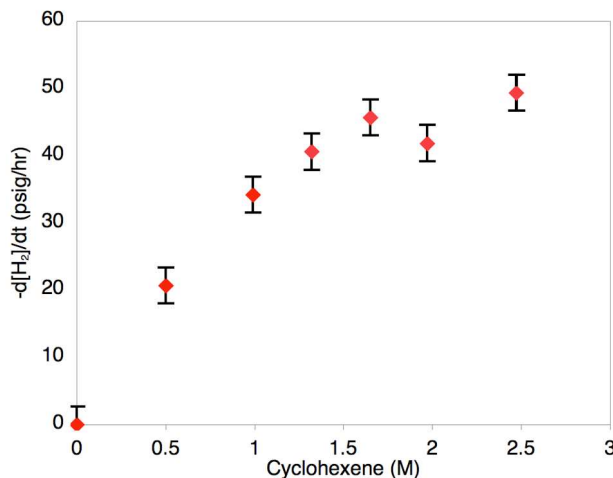


Figure S4. Cyclohexene dependent plots for the Ir(0)_{~900}/γ-Al₂O₃ heterogeneous nanoparticle catalyst formation reaction. The Figure shows that the rate of the Ir(0)_{~900}/ γ-Al₂O₃ heterogeneous nanoparticle formation reaction is independent of the cyclohexene concentration at 1.65 M, the amount of cyclohexene experimentally used

The Cyclohexene Reporter Reaction: Correcting the k_2 Observed Rate Constant for the Reporter Reaction Stoichiometry Factor

To get quantitative agreement between the observed rate constant $k_{2(\text{curve fit})}$ obtained by the cyclohexene reporter reaction and the cyclooctane GLC kinetic monitoring methods, a mathematically required correction factor is needed. The appropriate equation and correction factor derived before^{ii,iii} is reproduced below. Scheme 3 in the main text (bottom reaction) dictates that rate equation for the cyclohexene reporter reaction is that expressed in equation S1. Starting with the rate-determining steps, k_1 and k_2 , and substituting the mass balance equation, $[B] = ([A]_0 - [A])$ we obtain the right hand side of equation S1.

$$-\frac{d[A]}{dt} = \frac{d[B]}{dt} = k_1[A] + k_2[A][B] = k_1[A] + k_2[A]([A]_0 - [A]) \quad (\text{S1})$$

Turning this into what is actually followed by the cyclohexene reporter reaction (that is we add ~1700 equivalents of cyclohexene per Ir) and with the known 1:1 cyclohexene-to-H₂ stoichiometry, one obtains the previously demonstrated equation S2.^{iv}

$$-\frac{d[A]}{dt} = \frac{d[B]}{dt} = -\frac{1}{\sim 1700} \frac{d[\text{cyclohexene}]}{dt} = -\frac{1}{\sim 1700} \frac{d[H_2]}{dt} \quad (\text{S2})$$

Through several lines of algebra equation S3 is obtained.ⁱⁱ

$$\begin{aligned}
-\frac{d[\text{cyclohexene}]}{dt} &= k_1[\text{cyclohexene}]_t \\
&+ \frac{k_2}{\sim 1700}[\text{hexene}]_t([\text{cyclohexene}]_0 - [\text{cyclohexene}]_t)
\end{aligned} \tag{S3}$$

Integrating Equation S1 and expressing it in exponential form yields the integrated rate equation used to fit the kinetic data to the F–W 2-step mechanism.

$$[A]_t = \frac{\frac{k_1}{k_2} + [A]_0}{1 + \frac{k_1}{k_2[A]_0} * \exp(k_1 + k_2[A]_0)t} \tag{S4}$$

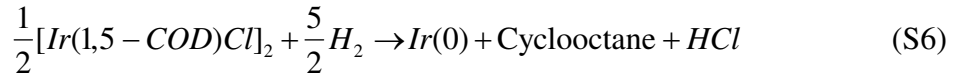
When the kinetic data are fit by equation S4, $k_{2(\text{curvefit})}$ is obtained, which needs to be corrected for the 1700:1 cyclohexene to Ir stoichiometry factor. This is done by taking $k_{2\text{curvefit}} = k_2/\sim 1700$ that is $\sim 1700 * k_{2(\text{curvefit})} = k_{2\text{corr}}$. Hence, when using the cyclohexene reporter reaction the obtained $k_{2(\text{curvefit})}$ rate constant needs to be corrected for the experimentally determined stoichiometry factor of 1700:1 (cyclohexene:Ir) as shown above.

Fitting the Cyclooctane Evolution Kinetics via the 2-step Mechanism

To fit the observed cyclooctane evolution kinetics a modified form of the integrated rate equation (S4) must be used. By substituting the mass balance equation $[A]_t = [A]_0 - [B]_t$ into equation S4, and for a clean stoichiometric $A \rightarrow B$ reaction, equation S5 results.

$$[B]_t = [A]_0 - \frac{\frac{k_1}{k_2} + [A]_0}{1 + \frac{k_1}{k_2[A]_0} \exp(k_1 + k_2[A]_0)t} \tag{S5}$$

In this case the obtained rate constant k_2 need not be corrected, as detailed below. Here we simplify the kinetic derivation by using the stoichiometry below, equation S6.



Again starting from the rate-determining step and setting $[A] = \frac{1}{2} [\text{Ir}(1,5-\text{COD})\text{Cl}]_2$ and $[B]_t = [\text{Ir}(0)]_t = [\text{cyclooctane}]_t$.

$$\frac{d[B]}{dt} = \frac{d[\text{Ir}(0)]}{dt} = \frac{d[\text{cyclooctane}]}{dt} = k_1[A]_t + k_2[A]_t[B]_t \tag{S7}$$

The following mass balance equations apply: (i) $[A]_0 = [\text{cyclooctane}]_\infty$ and (ii) $[A]_0 = [A]_t + [\text{Ir}(0)]_t = [A]_t + [\text{cyclooctane}]_t$. Thus (iii) $[A]_t = [\text{cyclooctane}]_\infty - [\text{cyclooctane}]_t$. Substituting (iii) and (ii) into S7 yields equation S8:

$$\frac{d[\text{cyclooctane}]}{dt} = k_1([\text{cyclooctane}]_{\infty} - [\text{cyclooctane}]_t) + k_2([\text{cyclooctane}]_{\infty} - [\text{cyclooctane}]_t)[\text{cyclooctane}]_t \quad (\text{S8})$$

Thus a plot of cyclooctane vs time, yields k_1 and k_2 rate constants *without any correction factors*.

Cyclooctane Evolution Kinetics for 1.96-wt% Ir(1,5-COD)Cl/ γ -Al₂O₃

The choice of Ir(1,5-COD)Cl/ γ -Al₂O₃ as a prototype precatalyst in the present work allows for an additional, very valuable kinetic monitoring method, one which functions as a direct control to check the results of the cyclohexene reporter reaction method. Specifically, using GLC we have directly monitored the cyclooctane evolution kinetics, of the Ir(1,5-COD)Cl/ γ -Al₂O₃ supported-nanoparticle heterogeneous catalyst formation reaction, Figure S5. The data were fit to equation S8, and the resultant rate constants are, $k_{1GLC} = 1.2(2) \times 10^{-3}$ and $k_{2GLC} = 1.2(2) \times 10^4 \text{ h}^{-1} \text{ M}^{-1}$. The quantitative agreement (within experimental error) between the rate constants obtained by the two methods, and post the mathematically required correction factor for the reporter-reaction method, offers *compelling evidence that both methods are correctly monitoring the same process in real time*, namely the Ir(0)_{~900}/ γ -Al₂O₃ supported-nanoparticle heterogeneous catalyst formation reaction.

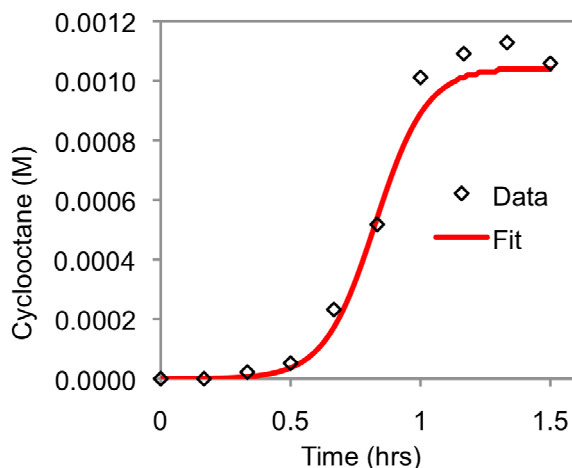


Figure S5. Cyclooctane evolution kinetics for the formation of Ir(0)_{~900}/ γ -Al₂O₃. The black diamonds are the experimental data and the blue line is the fit to the 2-step mechanism.

TEM Imaging, Corresponding Particle Size Histogram and Cyclooctane Evolution Kinetics for the Ir(0)_n/Al₂O₃ Supported-Nanoparticle Heterogeneous Catalyst Formation when Cyclohexene is not Present

In the synthesis of polyoxoanion Ir(0)_n stabilized nanoclusters in acetone, Ir(0)_{~300} nanoclusters form when cyclohexene is present, but larger Ir(0)_{~900} nanoclusters are formed in the absence of cyclohexene but still under H₂ as the reducing agent.^{iv,v} Hence

it was of interest to see if cyclohexene has similar effects or not in the present supported-nanoparticle system.

An $\text{Ir}(0)_n/\text{Al}_2\text{O}_3$ catalyst was therefore synthesized under the identical standard reaction conditions described above, except without cyclohexene present. A TEM of the resultant products is shown in Figure S6; on average 3.1 ± 0.5 nm nanoclusters are observed, and with the corresponding histogram shown in Figure S6. The corresponding particle size histogram for $\text{Ir}(0)_{\sim 1100}/\gamma\text{-Al}_2\text{O}_3$. Their size is within error of the 2.9 ± 0.4 nm ($\text{Ir}(0)_{\sim 900}/\gamma\text{-Al}_2\text{O}_3$) products when cyclohexene is present; hence cyclohexene plays little to no role in the observed $\text{Ir}(0)_n/\gamma\text{-Al}_2\text{O}_3$ supported-nanoparticle heterogeneous catalyst product.

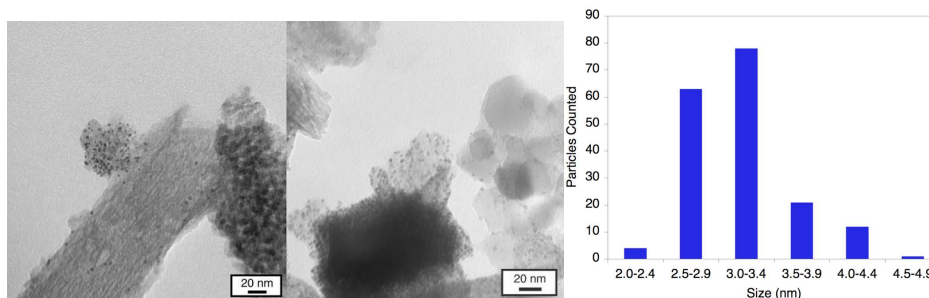


Figure S6. TEM imaging of the $\text{Ir}(0)_{\sim 1100}/\gamma\text{-Al}_2\text{O}_3$ supported-nanoparticle catalyst formed when cyclohexene is absent during the synthesis and the corresponding particle size histogram revealing 3.1 ± 0.5 nm nanoparticles.

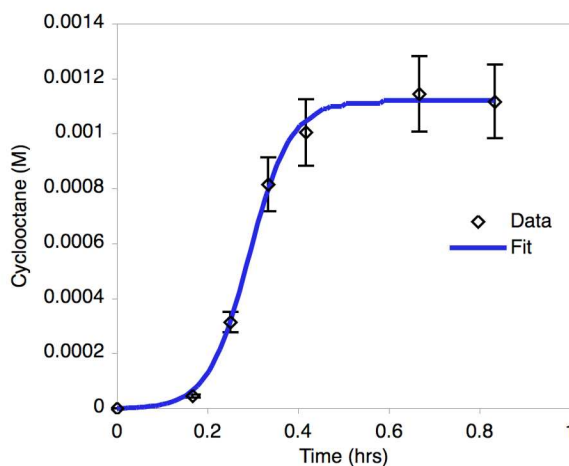


Figure S7. Cyclooctane evolution kinetics starting from the $\text{Ir}(1,5\text{-COD})\text{Cl}/\gamma\text{-Al}_2\text{O}_3$ precatalyst with the olefin cyclohexene not present. The black diamonds are the experimental data and the blue line is the fit to the 2-step mechanism.

To confirm this result, the cyclooctane evolution kinetics were monitored, and are shown in Figure S7 along with a fit to the 2-step mechanism. The resultant rate constants without the cyclohexene present, $k_{1\text{GLC}} = 3.5(2) \times 10^{-2} \text{ h}^{-1} \text{ M}^{-1}$ and $k_{2\text{GLC}} = 3.9(2) \times 10^4 \text{ h}^{-1} \text{ M}^{-1}$, are within error of those when cyclohexene is present ($k_{1\text{GLC}} = 1.2(2) \times 10^{-3} \text{ h}^{-1}$ and $k_{2\text{GLC}} = 1.2(2) \times 10^4 \text{ h}^{-1} \text{ M}^{-1}$).^{vi}

Confirming the Molecularity ($[A]^1$) of Nucleation, $A \rightarrow B$, Starting with $\text{Ir}(1,5\text{-COD})\text{Cl}/\gamma\text{-Al}_2\text{O}_3$

A series of precatalysts from 1.0-3.85-wt% were made following as described in the experimental section of the main text (Pre-Catalyst Preparation: $\text{Ir}(1,5\text{-COD})\text{Cl}/\gamma\text{-Al}_2\text{O}_3$). In each case the nucleation rate ($-\text{d}[A]/\text{dt}$) was taken once the H_2 uptake was ≥ 0.05 psig (albeit arbitrarily, but consistently and as precededⁱⁱ).

The \ln/\ln plot of the nucleation rate ($-\text{d}[A]/\text{dt}$ vs. $\text{Ir-wt}\%$) shown in Figure S8 is linear and reveals a slope of 1.01, that is 1.0 within experimental error and further verifying the $[A]^1$ molecularity of the $A \rightarrow B$ nucleation step of the 2-step mechanism.

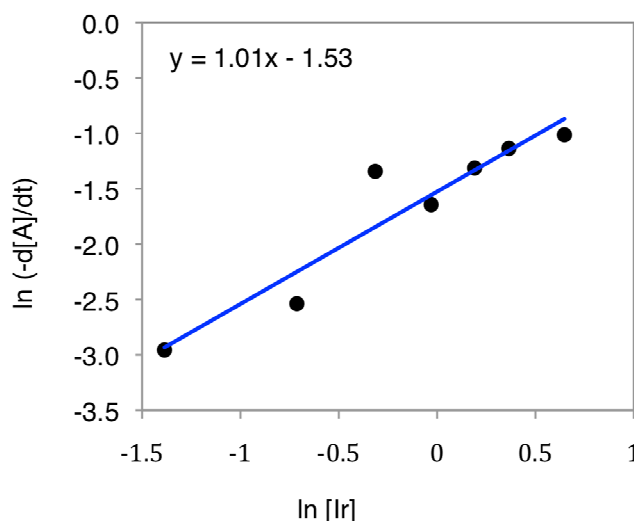


Figure S8. The \ln/\ln plot revealing first order kinetics for the nucleation step $A \rightarrow B$, starting with $\text{Ir}(1,5\text{-COD})\text{Cl}/\gamma\text{-Al}_2\text{O}_3$.

References

- (i) Aiken III, J. D.; Finke, R. G. *J. Am. Chem. Soc.* **1998**, *120*, 9545-9554.
- (ii) Watzky, M. A.; Finke, R. G. *J. Am. Chem. Soc.* **1997**, *119*, 10382-10400.
- (iii) Widegren, J. A.; Aiken III, J. D.; Ozkar, S.; Finke, R. G. *Chem. Mater.* **2001**, *13*, 312-324.
- (iv) Lin, Y.; Finke, R. G. *J. Am. Chem. Soc.* **1994**, *116*, 8335-8353.
- (v) Lin, Y., R.G. Finke, *Inorg. Chem.* **33** (1994) 4891-4910.
- (vi) The reporter $k_{1\text{GLC}}$ and $k_{2\text{GLC}}$ error bars are only derived from the non-linear least squares fit to the F-W 2-step mechanism, and do not correspond to the true experimental error inherent to the nucleation and growth kinetics. The true error bars for the supported-nanoparticle heterogeneous catalyst formation reaction are more accurately reflected in the reported k_1 value of $\sim 10^{-3.4(5)}$ and $k_{2\text{corr}} = 1.6(2) \times 10^4 \text{ h}^{-1} \text{ M}^{-1}$ obtained

from multiple runs via the cyclohexene reporter reaction kinetics (for references and more discussion, see the main text).